Functional Diversity of Signaling Pathways through G Protein–Coupled Receptor Heterodimerization with a Species-Specific Orphan Receptor Subtype

Tsubasa Sakai,[1] Masato Aoyama,[1] Takehiro Kusakabe,[2] Motoyuki Tsuda,[3] and Honoo Satake*[,1]

[1]Division of Biomolecular Research, Suntory Institute for Bioorganic Research, Osaka, Japan

[2]Department of Biology, Faculty of Science and Engineering, Konan University, Hyogo, Japan

[3]Laboratory of Functional Biology, Kagawa School of Pharmaceutical Sciences, Tokushima Bunri University, Kagawa, Japan

***Corresponding author:** E-mail: satake@sunbor.or.jp.

Associate editor: William Jeffery

Abstract

Gonadotropin-releasing hormones (GnRHs) play pivotal roles in control of reproduction via a hypothalamic–pituitary–periphery endocrine system and nervous systems of not only vertebrates but also invertebrates. GnRHs trigger several signal transduction cascades via GnRH receptors (GnRHRs), members of the G protein–coupled receptor (GPCR) family. Recently, six GnRHs (tunicate GnRH [tGnRH]-3 to tGnRH-8) and four GnRHRs (*Ciona intestinalis* [Ci]-GnRHR1 to GnRHR-4), including a species-specific paralog, Ci-GnRHR4 (R4) regarded as an orphan receptor or nonfunctional receptor, were identified in the protochordate, *C. intestinalis*, which lacks the hypothalamic–pituitary system. Here, we show novel functional modulation of GnRH signaling pathways via GPCR heterodimerization. Immunohistochemical analysis showed colocalization of R1 and R4 in test cells of the ascidian ovary. The native R1–R4 heterodimerization was detected in the *Ciona* ovary by coimmunoprecipitation analysis. The heterodimerization in HEK293 cells cotransfected with R1 and R4 was also observed by coimmunoprecipitation and fluorescent energy transfer analyses. Binding assay revealed that R4 had no affinity for tGnRHs, and the heterodimerization did not alter the binding affinity of R1 to the ligands. The R1–R4 elicited 10-fold more potent Ca^{2+} mobilization than R1 exclusively by tGnRH-6, although R1-mediated cyclic AMP production was not affected by any of tGnRHs via the R1–R4 heterodimer. Moreover, the R1–R4 heterodimer potentiated translocation of both Ca^{2+}-dependent protein kinase C-α (PKCα) by tGnRH-6 and Ca^{2+}-independent PKCζ by tGnRH-5 and tGnRH-6, eventually leading to the upregulation of extracellular signal-regulated kinase (ERK) phosphorylation compared with R1 alone. These results provide evidence that the species-specific GnRHR orphan paralog, R4, serves as an endogenous modulator for the fine-tuning of activation of PKC subtype–selective signal transduction via heterodimerization with R1 and that the species-specific GPCR heterodimerization, in concert with multiplication of tGnRHs and Ci-GnRHRs, participates in functional evolution of neuropeptidergic GnRH signaling pathways highly conserved throughout the animal kingdom.

Key words: GnRH, GPCR heterodimerization, orphan GPCR, evolution, *Ciona intestinalis*.

Research article

Introduction

Gonadotropin-releasing hormones (GnRHs) are hypothalamic decapeptides that regulate the hypothalamic–pituitary–gonadal axis in vertebrates and essentially conserve the consensus sequences of pyro-Glu[1]-His/Tyr[2]-Trp[3]-Ser[4], Gly[6], Pro[9]-Gly[10]-NH_2 across animal species, although their species-specific paralogous forms have also been determined (Kah et al. 2007; Millar et al. 2008). For example, tetrapods possess two forms of GnRH, GnRH-I and GnRH-II (Kah et al. 2007; Millar et al. 2008), whereas teleosts and lampreys have three forms (Kavanaugh et al. 2008). Moreover, the *gnrh-II* gene is not present in certain mammalian species, such as rodents and chimpanzee (Kah et al. 2007; Millar et al. 2008). The endogenous receptors, GnRH receptors (GnRHRs), belong to the class A G protein–coupled receptor (GPCR) family and elevate inositol triphosphate (IP_3) and intracellular calcium ions (Shacham et al. 2001). Type I GnRHRs, which completely lack a C-terminal tail region, are restricted to certain mammalian species, that is, the human, rodent, and cow. Type-II GnRHRs, which bear a C-terminal tail, are widely distributed in almost all vertebrates (Kah et al. 2007; Millar et al. 2008), whereas the type-II *gnrhr* gene is silenced due to a deletion of functional domains or interruption of full-length translation by the presence of a stop codon in the human, chimpanzee, cow, and sheep (Kah et al. 2007; Millar et al. 2008). In mammals, type-I and type-II GnRHRs are selective to GnRH-I and GnRH-II, respectively (Shacham et al. 2001). In contrast, nonmammalian vertebrate GnRHRs are devoid of selectivity for the cognate GnRHs (Ando and Urano 2005). These findings indicate molecular and functional divergence of GnRHergic systems, although the central roles of GnRHs or their evolutionarily related peptides (e.g., insect and nematode adipokinetic hormones) in the control of reproduction are conserved throughout all known animal species (Millar et al. 2004; Satake and Kawada 2006; Tsai and Zhang 2008; Lindemans et al. 2009).

Recently, six GnRH forms (tunicate GnRH [tGnRH]-3 to tGnRH-8) (Adams et al. 2003) and four GnRHR subtypes (*Ciona intestinalis* GnRH4 to GnRH4) (Tello et al. 2005) were

identified in the protochordate, *C. intestinalis*, which lacks a hypothalamic–pituitary–periphery endocrine system essentially conserved in vertebrates (Campbell et al. 2004; Satake and Kawada 2006). Ci-GnRHR2 (R2), R3, and, R4 are ascidian-specific paralogs of R1 generated via gene duplication (Tello et al. 2005). Only R1, like the vertebrate GnRHRs, activates IP_3 generation in response to tGnRH-6, whereas R2 and R3, with their ligand selectivity, exclusively stimulate cyclic AMP (cAMP) production in response to multiple tGnRHs. In contrast, no tGnRHs activate R4, suggesting R4 to be an orphan or nonfunctional receptor (Tello et al. 2005).

Notably, heterodimerization of several GPCRs with their orphan receptor subtypes results in modulation of ligand-binding affinities, cell signaling, and/or receptor desensitization of the corresponding protomers (Levoye, Dam, Ayoub, Guillaume, Couturier, et al. 2006; Levoye, Dam, Ayoub, Guillaume, Jockers, et al. 2006; Milasta et al. 2006). In the present study, we show novel ligand-selective regulation of protein kinase C (PKC) subtype activation mediated via GPCR heterodimerization. The present data provide evidence that the orphan GnRHR paralog R4 is responsible for "fine-tuning" of the GnRHergic signaling pathways via heterodimerization with R1 and that GPCR heterodimerization with its orphan receptor paralog is involved in the functional diversity and species-specific regulation of GnRHergic systems.

Materials and Methods

Antibodies

An 11-amino acid peptide of the extracellular domain 3 of R1 (YDWFIRYEDHT-NH2) conjugated with keyhole limpet hemocyanin and a 13-amino acid peptide of the extracellular domain 3 of R4 (WFNEQHIERLPEG-NH2) with keyhole limpet hemocyanin were used as respective antigens (Operon Biotechnologies, Tokyo, Japan). An R1 antibody and an R4 antibody were raised in rabbit and chicken, respectively, by Operon Biotechnologies. Western blotting analysis indicated that the anti-R1 antibody recognized endogenous R1 expressed in the *Ciona* ovary and recombinant R1 transfected into HEK293MSR cells (supplementary fig. S1, Supplementary Material online). Likewise, the anti-R4 antibody recognized recombinant R4 and endogenous receptors in the ovary (supplementary fig. S1, Supplementary Material online).

Immunohistochemistry

Preparation and immunostaining of *Ciona* ovary sections were performed as previously described (Satake et al. 2004; Aoyama et al. 2008). No specific immunostaining was observed using a secondary antibody alone or the preabsorbed R1 antibody or R4 antibody. The preabsorbed R1 antibody or R4 antibody (1:1000) was prepared by incubation with the antigen peptides, which were used for generation of the respective antibody (YDWFIRYEDHT-NH_2 for the R1 antibody and WFNEQHIERLPEG-NH_2 for the R4 antibody) at a final concentration of 10^{-5} M for overnight at 4 °C.

Transfections and Cells

HEK293MSR cells were grown under 5% CO_2 in Dulbecco's modified eagle medium (DMEM) medium supplemented with 10% heat-inactivated fetal bovine serum at 37 °C. R1 or R3 was cloned into a pcDNA4/V5 vector and R4 was cloned into a pcDNA6/myc vector, respectively (Invitrogen, Carlsbad, CA), and transfected into HEK293MSR cells using Targefect F-1 reagent (Targeting Systems, Santee, CA). The stable transfectants were selected in the medium containing 20 μg/ml blasticidin and/or 400 μg/ml zeocin.

Coimmunoprecipitation and Western Blotting

The *Ciona* ovary or pellets of HEK293MSR transfectants were homogenized in 10 mM Tris, 0.1 mM ethylenediaminetetraacetic acid (EDTA), and pH 7.4 (Tris–ethylenediaminetetraacetic acid buffer) with protease inhibitors, and the membrane fractions were obtained by centrifugation at 50,000 × g for 60 min. The membrane fractions were then lysed in radioimmunoprecipitation assay buffer (Thermo Scientific, Waltham, MA) for 1 h at 4 °C on a rotating wheel. The resultant supernatant of the ovary or HEK293MSR transfectants was mixed with 2 μg of anti-R1 rabbit antibody or 5 μg of anti-Myc affinity agarose (Sigma, St Louis, MO) overnight at 4 °C on a rotating wheel, respectively. The anti-R1 antibody–antigen complexes were precipitated by protein G–linked Sepharose (GE Healthcare, Buckinghamshire, United Kingdom). The denatured coimmunoprecipitation products were subjected to sodium dodecyl sulfate analysis and electroblotted onto polyvinylidene fluoride membranes. Immunoreactivity was detected with anti-R4 antibody and corresponding secondary antibody or a horseradish peroxidase–linked anti-V5 antibody (Invitrogen). Bands were visualized by a chemiluminescent detection system (ECL detection kit; GE Healthcare).

Fluorescence Resonance Energy Transfer Imaging

For fluorescence resonance energy transfer (FRET) analysis, receptor cDNAs for R1 and R4 were amplified by polymerase chain reaction to generate stop codon–free fragments. The fragments were then subcloned in frame into the 5′-end of the CFP and YFP vectors, respectively. Cells were cultured on glass bottom 35-mm tissue culture dishes and transfected with expression vectors for appropriate CFP/YFP fusion Ci-GnRHRs. Cells were visualized using confocal laser microscopy, FLUOVIEW FV1000 (Olympus, Tokyo, Japan). CFP and YFP were excited with the 458- and 515-nm lines of an argon laser, respectively. The emitted fluorescence was collected at 475–500 nm for CFP and 530–630 nm for YFP. Cells expressing either R1-fused CFP (R1-CFP) or R4-fused YFP (R4-YFP) alone or coexpressing these two constructs were excited with the 458-nm line, and the emitted fluorescence was collected at 530–630 nm for FRET analysis.

Radioligand Binding

[^{3}H]-tGnRH-6 (33 Ci/mmol) was prepared by the custom order service of GE Healthcare. Saturation binding assays were performed on intact stably transfected HEK293MSR cells with [^{3}H]-labeled tGnRH-6. For saturation binding assays, 5.0×10^4 cells were seeded into 96-well plates in 100 μl medium; these were grown for overnight at 37 °C in 5% CO_2. Cells were then replaced once in 50 μl DMEM,

followed by incubation with increasing concentrations of [^{3}H]-tGnRH-6 (1–100 nM) in 50 µl of assay buffer (50 mM Tris, 1 mM EDTA, 3 mM $MgCl_2$, and pH 7.4) for 3 h at 4 °C. Nonspecific binding was determined using cells incubated with both [^{3}H]-labeled tGnRH-6 and 10 µM unlabeled tGnRH-6. After 3-h incubation, cells were washed twice with 150 µl ice-cold phosphate-buffered saline (PBS), solubilized, and subjected to scintillation counting. All total binding samples were run in triplicate, nonspecific binding samples were run in duplicate, and each independent experiment was repeated three times. Data were analyzed using Prism (GraphPad, La Jolla, CA).

Competitive binding properties of tGnRH-3, tGnRH-5, and tGnRH-6 were performed using the transfected cells. Cells were prepared as described above; however, the [^{3}H]-labeled tGnRH-6 concentration was held constant at 25 nM, with either assay buffer (total binding) or increasing concentrations of cold competing ligand in assay buffer (ranging from 10^{-10} to 10^{-5} M) in 100 µl total volume for 3 h at 4 °C. Cells were washed and processed as described above. All samples were run in triplicate, in three independent experiments.

Determination of intracellular Ca^{2+} and cAMP levels

Real-time fluorescent kinetics for Ca^{2+} mobilization using a Ca3 kit (Molecular Devices, Sunnyvale, CA) and end point observation of cAMP production using CatchPoint™ Cyclic AMP Assay Kit (Molecular Devices) were performed on FlexStation II according to the manufacturer's instruction.

Measurement of ERK1/2 Activation

Phosphorylation of ERK1/2 in Ci-GnRHRs-expressing HEK293MSR cells was measured by Western blotting. Total and phosphorylated ERKs were extracted from the HEK293MSR transfectants after stimulation with 5 nM tGnRH-6 or 25 nM tGnRH-5 and was detected by ECL detection kit (GE Healthcare) using polyclonal rabbit anti-total ERK1/2 and rabbit anti-pp ERK1/2 (Cell Signaling Technology, Danvers, MA) on duplicate membranes according to manufacturer's instruction. The bands were scanned and quantified by densitometry.

PKC Translocation Assay

Cells on a collagen type I–coated glass slide (Becton Dickinson, Bedford, MA) were incubated in serum-free medium for 15 h. After stimulation with 5 nM tGnRH-6 or 25 nM tGnRH-5, cells were fixed in 4% formaldehyde for 15 min and permeabilized with 0.2% Triton-X in PBS for 30 min. The slide glasses were incubated with a blocking medium followed by treatment with the PKC subtype–specific antibodies (Santa Cruz Biotechnology, Santa Cruz, CA). Alexa 488–conjugated goat anti-rabbit immunoglobulin G secondary antibody (Invitrogen) was used for visualization. Stained PKCs in Ci-GnRHRs-expressing cells were assessed on four images/coverslip, each of which contained an average of eight cells, using confocal microscopy, FLUOVIEW FV1000, and FV10-ASW1.7 software (Olympus). Results are expressed as the ratio of the immunostained intensities on plasma membranes to cytosol.

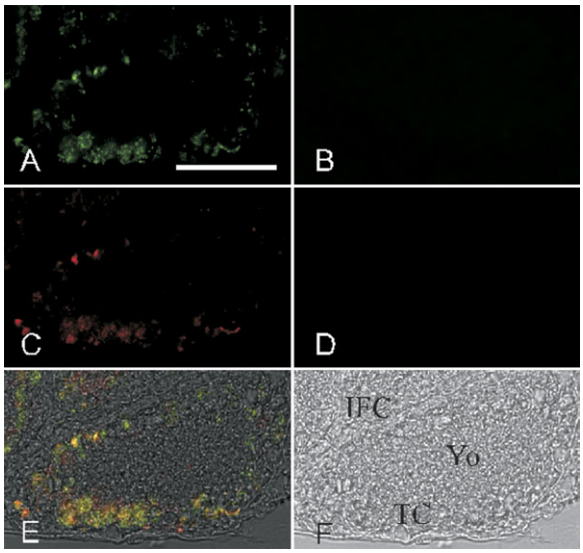

Fig. 1. Localization of R1 and R4 in the ovary. Immunostaining using the R1- or R4-specific antibody followed by treatment with Alexa 488–conjugated secondary antibody (green for R1, panel A) and Alexa 568–conjugated secondary antibody (red for R4, panel C). No specific immunostaining was observed using the preabsorbed R1 antibody (*B*) and the preabsorbed R4 antibody (*D*). The merged image clarifies the colocalization of R1 and R4 in test cells in the ovary (*E*). The pictures are representative of three different experiments. (*F*) Bright-field view of the gonad. IFC, inner follicular cell; Yo, Yolk. Scale bar: 50 µm.

Statistical Analysis

Results are expressed as means ± standard error mean for indicated number of observations. Data were analyzed by one-way analysis of variance with Dunnett error protection. Differences were accepted as significant for $P < 0.05$.

Results

Detection of the R1–R4 Heterodimer

A prerequisite for the formation of R1–R4 heterodimers is their coexpression in the same cells. The immunoreactivity of R1 was detected exclusively in test cells residing inside of inner follicles of oocytes (fig. 1), which are believed to be involved in oocyte growth (Aoyama et al. 2008). The immunoreactivity of R4 was largely colocalized with that of R1 (fig. 1). No positive signals were observed when antigen-absorbed antibodies were applied, confirming the specificity of the immunostaining (fig. 1*B* and *D*). Coimmunoprecipitation of the ovary membrane using anti-R1 and anti-R4 antibodies detected the specific bands corresponding to a R1 and R4 in the *Ciona* ovary at 100 kDa (fig. 2*A*). In combination, these data provide evidence that R4 forms a heterodimer with R1 in the *Ciona* ovary. To further examine the interaction between R1 and R4, we performed coimmunoprecipitation of V5-tagged R1 and Myc-tagged R4 stably transfected into HEK293 MSR cells without tGnRHs ligand administration. Myc-tagged R4 in the

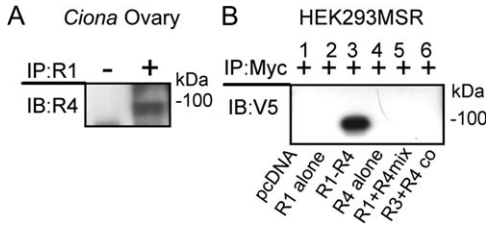

FIG. 2. Heterodimerization between R1 and R4. (*A*) Detection of R1–R4 heterodimer in the plasma membrane prepared from the *Ciona* ovary. The ovary membrane was immunoprecipitated with anti-R1 antibody and then immunoblotted with anti-R4 antibody. (*B*) R1–R4 heterodimer was also detected on the membrane of HEK293MSR cells expressing both V5-tagged R1 and Myc-tagged R4. The R1, R4, and R1–R4 transfectants were prepared, and immunoprecipitation with anti-Myc affinity agarose was followed by immunoblotting with anti-V5 antibody detecting the R1–R4 heterodimer (lane 3). No corresponding bands were detected in any membrane fractions from the R1 or R4 transfectants (lanes 2 and 4), an immunoprecipitate mixture of the membrane fractions separately prepared from the cells expressing each receptor (lane 5) or the fraction from R3- and R4-coexpressing transfectant (lane 6).

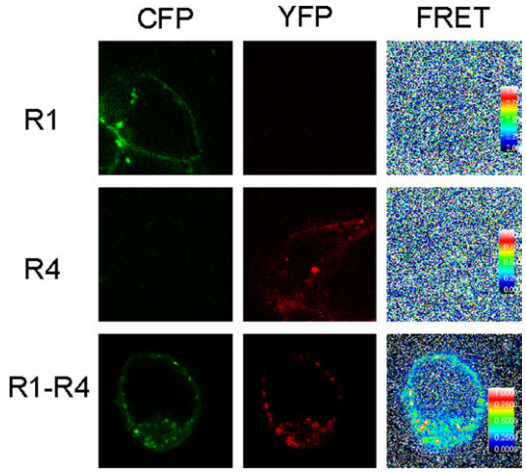

FIG. 3. FRET imaging constitutive R1–R4 heterodimeric interactions. R1-CFP (upper panels) and R4-YFP (middle panels) were expressed individually or coexpressed (lower panels) in HEK293MSR cells. Individual cells were imaged. Left-hand panels, CFP; center panels, YFP; right-hand panels, FRET.

membrane fraction was immunoprecipitated with monoclonal anti-Myc antibody, followed by western blotting of the immunoprecipitate using a monoclonal anti-V5 antibody. As shown in figure 2*B*, the specific band corresponding to an R1–R4 heterodimer was detected at 100 kDa only in cells coexpressing both receptors (fig. 2*B*, lane 3) but not in cells expressing the empty vector (lane 1) and either protomer (lane 2 and 4). Moreover, no bands were detectable under the identical condition in an immunoprecipitate mixture of the membrane fractions separately prepared from the cells expressing each receptor (fig. 2*B*, lane 5), excluding the possibility that the R1–R4 heterodimer resulted from artifacts. Additionally, coimmunoprecipitation of V5-tagged R3 and Myc-tagged R4 generated no bands (fig. 2*B*, lane 6), confirming the specificity of the heterodimerization between R1 and R4. In combination, these data provide evidence that R4 specifically forms a constitutive heterodimer with R1. The constitutive R1–R4 heterodimer in living HEK293MSR cells transfected with both the receptors was also confirmed by FRET analysis, using cells expressing either R1-CFP or R4-YFP alone or coexpressing these two constructs. FRET signals were obtained from the R1-CFP– and R4-YFP–coexpressing cells but not from R1-CFP– or R4-YFP–expressed cells (fig. 3). In combination, these data verified that R4 specifically forms a heterodimer with R1.

Effects of the R1–R4 Heterodimer on Intracellular Signaling

Reverse transcriptase–polymerase chain reaction and mass spectrometry analyses revealed that tGnRH-3, tGnRH-5, and tGnRH-6 (pQHWSYEFMPG-NH_2, pQHWSYEYMPG-NH_2, and pQHWSKGYSPG-NH_2, respectively), encoded by the *Ci-gnrh1* gene, are major active GnRH isoforms in the adult ascidian, whereas the *Ci-gnrh2* gene encoding tGnRH-4, tGnRH-7, and tGnRH-8 is not expressed in any adult tissues (Kawada et al. 2009). Consequently, we evaluated the activities of tGnRH-3, tGnRH-5, and tGnRH-6 at Ci-GnRHRs. Furthermore, intracellular Ca^{2+} mobilization is triggered exclusively by R1 bound to tGnRH-6 (Tello et al. 2005). Notably, as shown in figure 4*A* and *B*, tGnRH-6 exclusively exhibited ≈10-fold more potent Ca^{2+} mobilization (EC_{50} = 0.55 nM) in the HEK293MSR cells expressing R1–R4 than in the cells expressing R1 alone (EC_{50} = 6.92 nM), whereas no Ca^{2+} mobilization by tGnRH-3 or tGnRH-5 was detected in any receptor-expressing cells as previously reported (Tello et al. 2005). In addition, dose-dependent effects of R4 expression levels on Ca^{2+} mobilization by tGnRH-6 at R1 stably transfectant were detected (supplementary table S1 and fig. S2, Supplementary Material online). On the other hand, no alteration of cAMP production was detected in the R1- and R4-coexpressing cells compared with the R1-expressing cells (fig. 4*C* and *D*). Binding assays demonstrated that tGnRH-6 exhibited high affinity to R1 and the order of the affinity of tGnRH was tGnRH-6 > tGnRH-5 > tGnRH-3 (table 2 and fig. 5), whereas R4 had no affinity for tGnRHs (table 1 and fig. 5). Moreover, the R1–R4 heterodimer exhibited equivalent binding affinity for tGnRHs to R1 (tables 1 and 2 and fig. 5). Collectively, these results indicate that the heterodimerization elevates Ca^{2+} mobilization by tGnRH-6 without alteration in the ligand-binding affinity of R1.

ERK1/2 Phosphorylation and PKC Translocation by tGnRH via R1 or R1–R4

GnRHRs have been shown to induce ERK1/2 phosphorylation in mitogen-activated protein kinase (MAPK) pathways mainly via activation of PKCs in a Ca^{2+}-dependent or Ca^{2+}-independent fashion (Shacham et al. 2001). In cells expressing R1 alone, typical ERK1/2 phosphorylation was induced by 5 nM tGnRH-6, with the maximal effect at 5 min after ligand addition and the signal returned to the basal level

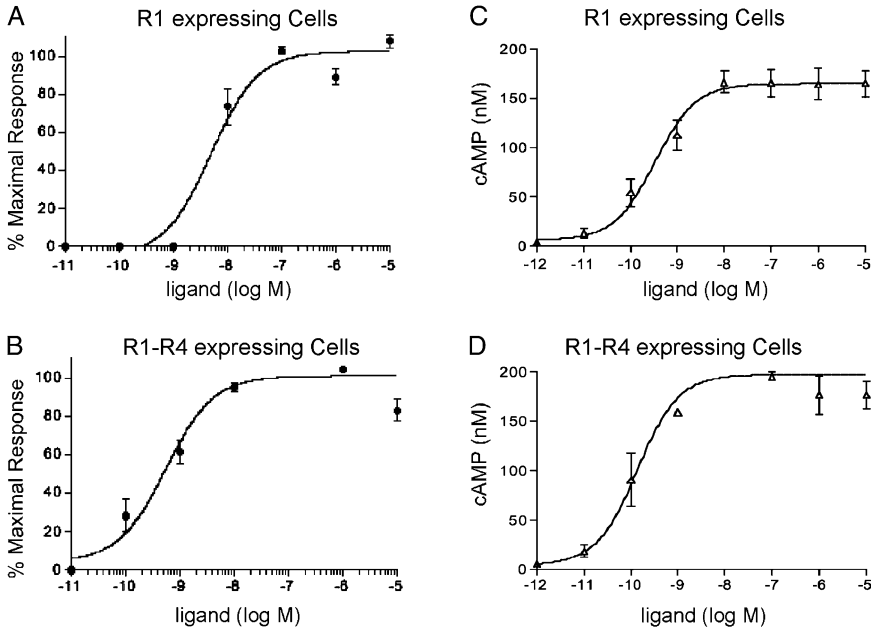

Fig. 4. Effect of the heterodimer on intracellular signaling. (*A* and *B*) Dose-response curves for calcium mobilization by tGnRH-6 (filled circles) at R1 (*A*) and R1–R4 (*B*) expressed in HEK293MSR cells. Fluorescent responses by 1 μM tGnRH-6 are taken as 100% activation. (*C* and *D*) Concentration-dependent cAMP production obtained by a fluorescence competitive immunoassay. Dose-response curves for tGnRH-6 (open triangles) on R1 (*C*) and R1–R4 (*D*) expressed in HEK293MSR cells. No alteration of cAMP production was detected in R1- to R4-expressing cells compared with R1-expressing cells. Results are shown as means ± standard error mean of three individual experiments.

within 15 min (fig. 6*A*). Intriguingly, a similar induction of ERK1/2 phosphorylation was observed by the addition of 25 nM tGnRH-5 (fig. 6*B*), which fails to elevate intracellular Ca^{2+}. ERK1/2 phosphorylation was not induced in cells expressing R1, R4, or R1–R4 by any other tGnRH, including tGnRH-3 (data not shown), which is encoded with tGnRH-5 and tGnRH-6 by *Ci-gnrh1* (Adams et al. 2003). The striking feature is that coexpression of R1 and R4 in HEK293MSR cells upregulated 3- and 5-fold more ERK1/2 phosphorylation by tGnRH-5 and tGnRH-6 than that of R1, respectively (fig. 6*A* and *B*). Administration of Gö6983, an inhibitor of PKCα, β, γ, δ, and ζ, resulted in a significant decrease in the ERK1/2 phosphorylation induced by tGnRH-5 or tGnRH-6 in R1 cells (41% and 40% of the inhibitor-untreated cells, respectively), confirming that the ERK1/2 phosphorylation by tGnRH-5 or tGnRH-6 via R1 is mediated largely by PKC subtypes. As depicted in figure 6*C* and *D*, the inhibition by Gö6983 was more dramatically enhanced in the heterodimer-expressing cells (13% and 20% of the inhibitor-untreated cells, respectively), indicating that the R1–R4 heterodimer–mediated upregulation of ERK1/2 phosphorylation is more closely dependent on PKC activation compared with R1 alone. Activation of PKCs resulted from their rapid translocation from the cytoplasm onto the plasma membrane (Kratzmeier et al. 1996; Farshori et al. 2003; Shah et al. 2003). We thus observed the translocation of Gö6983-sensitive PKC subtypes, namely PKCα, β, γ, δ, and ζ, in R1- or R1- to R4-expressing cells at 5 min after administration of either tGnRH-5 or tGnRH-6, revealing that PKCα was translocated by tGnRH-6 alone, and translocation of PKCζ was induced in response to tGnRH-5 and tGnRH-6 in the R1-expressing cells (fig. 7 and supplementary table S2, Supplementary Material online). These results are compatible with previous studies showing that GnRH induced translocation of PKCα (Farshori et al. 2003; Shah et al. 2003) and PKCζ (Kratzmeier et al. 1996). In addition, such magnitudes and subtype species of the translocated PKCs are compatible with those by mammalian GnRH signaling in various cell lines, excluding the possibility that these data are cell context specific (Kratzmeier et al. 1996; Shah et al. 2003). In the R1–R4 heterodimer–expressing cells, tGnRH-6 elicited 2-fold translocation of PKCα compared with R1-expressing cells (fig. 7 and supplementary table S2, Supplementary Material online). Likewise, the translocation of PKCζ in the R1–R4 heterodimer–expressing cells by tGnRH-5 and tGnRH-6 was 1.8- and 1.7-fold enhanced, respectively, compared with R1-expressing cells (fig. 7 and supplementary table S2, Supplementary Material online). These results provide evidence that the R1–R4 heterodimer induces more prominent translocation of PKCα by tGnRH-6 and PKCζ by tGnRH-5 and tGnRH-6.

Discussion

The present data verified that the heterodimerization of R1 with an orphan receptor paralog, R4, modulates PKC-mediated MAPK pathways regulated by R1 (fig. 8). Of particular significance is that the activation of specific PKC subtypes, eventually leading to ERK phosphorylation, is differentially upregulated by heterodimerization between a GnRH receptor and its orphan receptor paralog in a ligand-selective manner. To the best of our knowledge, this is the first characterization of the modulation of GnRH receptor–mediated signaling pathways (figs. 4 and 6) via

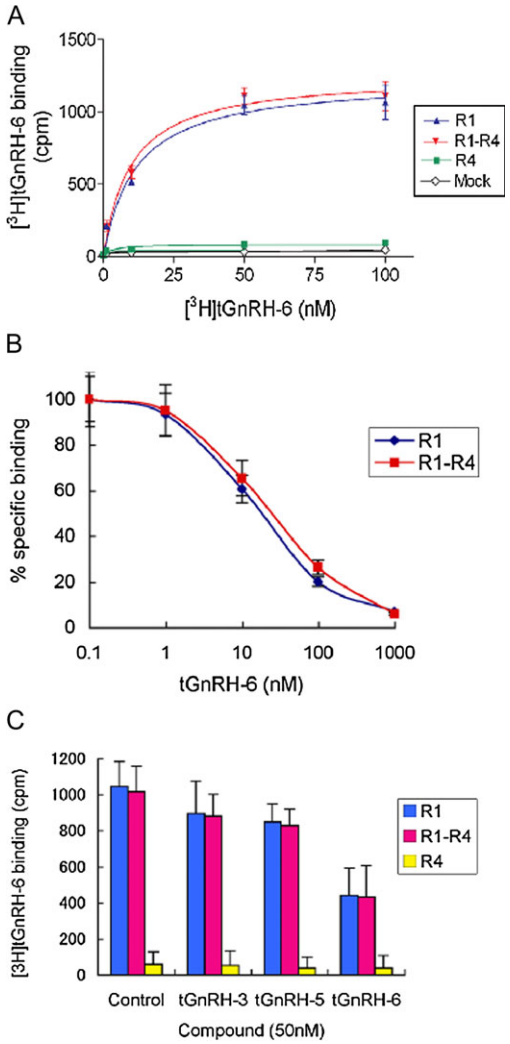

Fig. 5. Binding assays for R1 alone and R1–R4 heterodimer. (*A*) Saturation binding analysis of [^{3}H]-tGnRH-6 for R1, R1–R4, R4, or mock. R4 showed no binding to [^{3}H]-tGnRH-6, and R1–R4 heterodimer showed binding affinity to tGnRHs comparable with R1. Data are shown as means ± standard error mean (SEM) of three individual experiments. (*B*) Competitive binding analysis of [^{3}H]-tGnRH-6 with increasing concentrations of tGnRH-6. Data shown as means ± SEM ($n = 3$) of specific binding demonstrate that the R1–R4 heterodimer exhibited equivalent binding affinity for tGnRH-6 to R1. (*C*) tGnRH-3, tGnRH-5, and tGnRH-6 elicit competitive binding affinity to R1 and R1–R4 in the presence of [^{3}H]-tGnRH-6.

GPCR heterodimerization, modulatory effects of GPCR heterodimerization on PKC activation, and ligand-selective differential activation of PKC subtypes via GPCR heterodimerization (fig. 7). Moreover, the *Ciona* genome contains MAPK cascade-relevant orthologs, including phospholipase Cs, PKCα, PKCζ, and ERKs (Sasakura et al. 2003; Satou et al. 2003), and the R1–R4 heterodimer was detected in the *Ciona* ovary (fig. 1). Together, these results reveal a novel GPCR heterodimerization–directed regulation of the GnRHergic system. In addition, it is likely that R1 and R4 form a heterodimer with other GPCRs families, as seen in diverse GPCR heterodimers, given that distribution of R1 largely, but not completely, accorded with that of R4 in the ovary. Thus, our present study provides a valuable paradigm for functional diversity in essentially conserved signaling cascade via species-specific GPCR heterodimerization.

Table 1. Ligand-Binding Properties of R1, R1–R4 Heterodimer, and R4.

[^{3}H]-tGnRH-6 Binding					
K_d (nM)			B_{max} (fmol/well)		
R1	R1–R4	R4	R1	R1–R4	R4
29.7 ± 8.5	27.6 ± 9.4	ND	450.3 ± 47.4	492.1 ± 55.3	ND

Note.—The dissociation constant (K_d) and number of [^{3}H]-tGnRH-6-binding sites (B_{max}) were calculated by Scatchard analysis. The data are presented as the means ± standard error mean of three independent experiments performed in triplicate. ND, not detected.

One Ca^{2+}-dependent PKC subtype, PKCα, was activated exclusively by tGnRH-6 via R1, and the translocation was markedly potentiated by heterodimerization of R1 with R4 (fig. 7). These results are consistent with the second messenger assay showing that tGnRH-6 elicited 10-fold potent Ca^{2+} mobilization through the R1–R4 heterodimer compared with R1 alone (fig. 4). tGnRH-6 also enhanced a Ca^{2+}-independent PKC, PKCζ (fig. 7), indicating that tGnRH-6 is responsible for the activation of both Ca^{2+}-dependent and Ca^{2+}-independent MAPK pathways. Moreover, translocation of PKCζ was induced by tGnRH-5 (fig. 7), which does not exhibit any Ca^{2+} mobilization at R1 or R1–R4. These data indicate that R1 mediates the PKC activation pathways, which are differentially triggered by different tGnRH isoforms. In addition, R1-mediated cAMP production was not affected by the heterodimerization (fig. 4*C* and *D*). Furthermore, the inhibitory effects of Gö6983 on ERK phosphorylation via the Ci-GnRHRs (fig. 6*C* and *D*) demonstrated that activation of the two PKC subtypes plays a more important role in ERK phosphorylation via R1–R4 than via R1, given that ERK phosphorylation via R1–R4 is more potently suppressed by Gö6983 than ERK phosphorylation via R1 (fig. 6*C* and *D*). Collectively, these results lead to the conclusion that R4 specifically participates in the upregulation of the PKCα- and PKCζ-mediated MAPK pathways via heterodimerization with R1 (fig. 8).

R1–R4 heterodimerization did not alter the binding affinity of R1 to any of tGnRHs and its expression (fig. 5 and tables 1 and 2), although R4 modulated R1-triggered signaling cascades (figs. 4, 6, and 7). Furthermore, no alteration in expression of R1-CFP or R4-YFP was detected in the R1-CFP– and R4-YFP–coexpressing cells compared with the R1-CFP– or R4-YFP–expressing cells (fig. 3). In addition, no difference in internalization between the R1–R4 and

Table 2. The Half-Maximal Inhibitory Concentrations (IC_{50}) of tGnRH-3, tGnRH-5, and tGnRH-6.

[^{3}H]-tGnRH-6-Binding Affinity IC_{50} (nM)			
Ligands	R1	R1–R4	R4
tGnRH-3	130.7 ± 30.5	112.8 ± 40.6	>1,000
tGnRH-5	36.1 ± 11.3	32.4 ± 13.5	>1,000
tGnRH-6	7.5 ± 3.2	8.1 ± 3.6	>1,000

The data are presented as the means ± standard error mean of three independent experiments performed in triplicate.

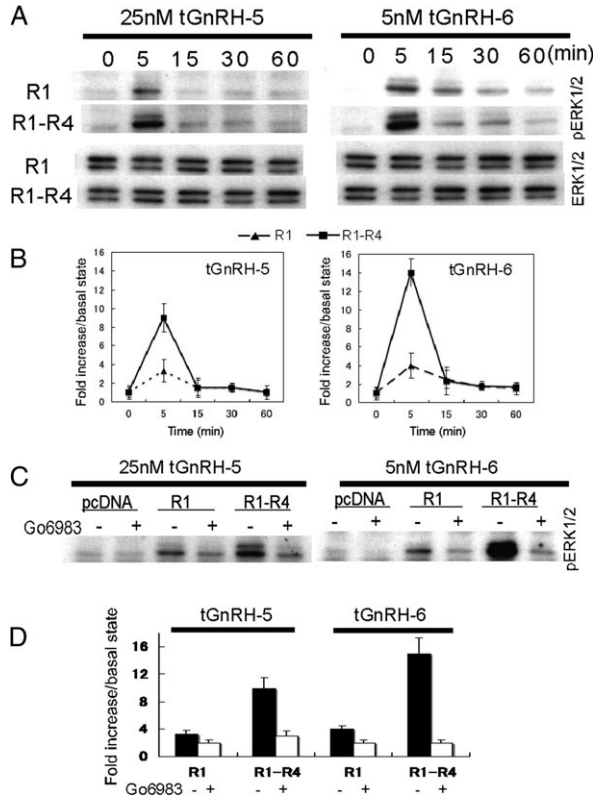

Fig. 6. Ci-GnRHR-mediated ERK1/2 activation in HEK293MSR cells–expressing R1 or R1–R4 were stimulated with 25 nM tGnRH-5 or 5 nM tGnRH-6. (*A*) Western blots for phosphorylated ERK1/2 via R1 (top) and R1–R4 (bottom) stimulated by tGnRH-5 or tGnRH-6 for 0–60 min, as indicated. (*B*) Results were quantified by densitometric analysis. The data were expressed as the fold ERK1/2 phosphorylation over the basal value at 0 min treated cells ($n = 3$ experiments). (*C*) ERK phosphorylation by tGnRH-5 or tGnRH-6 in R1-expressing cells was partially suppressed in the presence of 1 μM Gö6983, and the suppression in R1- to R4-expressing cells was more prominent than in R1-expressing cells. 0.1% dimethyl sulfoxide was administrated as control for the inhibitor. Cell expressing the empty vector indicated no ERK1/2 phosphorylation by administration of either tGnRH-5 or tGnRH-6. (*D*) Quantification of inhibitory effect of Gö6983 is shown. Results are shown as means ± standard error mean of three individual experiments.

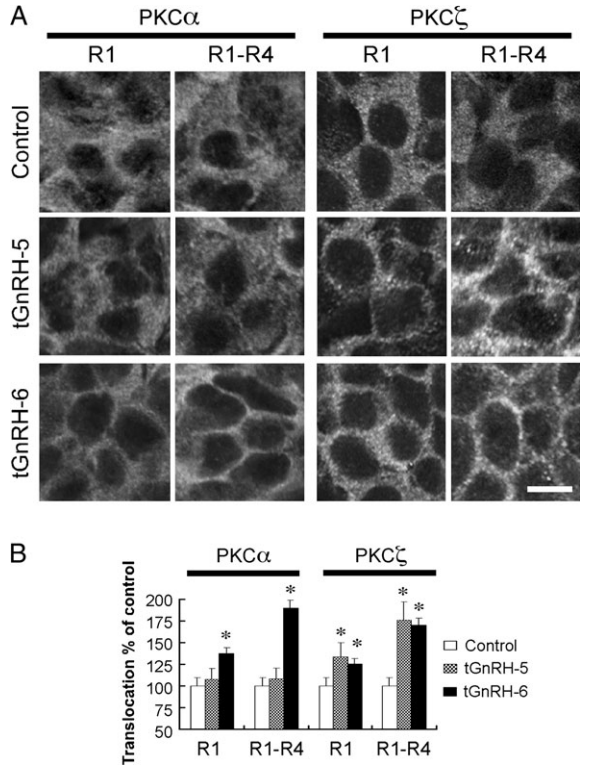

Fig. 7. Translocation of PKCα and PKCζ induced by 25 nM tGnRH-5 or 5 nM tGnRH-6 to the plasma membrane of HEK293MSR cells–expressing R1 or R1–R4. Cells stably transfected with R1 or R1–R4 were treated with tGnRHs or PBS as control for 5 min before fixation. (*A*) Representative immunostaining using a PKCα (sc-208; Santa Cruz Biotechnology) and PKCζ (sc-216) antibodies is shown ($n = 3$ experiments). Scale bar: 10 μm. (*B*) The ratio of intensity of stained PKCs on plasma membranes to cytosol was quantified using confocal microscopy and FV10-ASW1.7 software (Olympus). Results are shown as means ± standard error mean of three individual experiments. *$P < 0.05$ compared with the corresponding control group.

R1 was observed (data not shown). These data indicated that the modulation of the R1-mediated signaling cascades via heterodimerization with R4 is attributable to alterations neither in the ligand-binding affinity nor in the expression on the cell membrane. Recently, there has been a growing body of evidence that GPCRs assume multiple active conformations induced by agonists, leading to the activation of various different signaling pathways (Caunt et al. 2006; Dobkin-Bekman et al. 2006; Milligan and Smith 2007; Satake and Sakai 2008). These findings indicate that different active conformations of R1 are induced by tGnRH-5 and tGnRH-6 and that such distinctly different active conformations, leading to differential activation of PKCα and PKCζ, are enhanced via heterodimerization with R4. In other words, R4 is highly likely to stabilize several forms of the active conformations of R1 as an endogenous allosteric modulator. In mammals, several orphan receptors have been reported to act as a heterodimer unit: the orphan receptors Mas-related gene E and GPR50 heterodimerize with the β-alanine receptor MrgD and melatonin receptors, respectively (Levoye, Dam, Ayoub, Guillaume, Couturier, et al. 2006; Levoye, Dam, Ayoub, Guillaume, Jockers, et al. 2006; Milasta et al. 2006). These findings are consistent with the present data and suggest that several "orphan" receptors serve as functional modulators of nonorphan GPCRs via heterodimerization rather than as signal transducers directly activated through specific interactions with unidentified ligands. Also of interest is the regulation of the expression of R1–R4 heterodimer. The immunoreactivity of R4 in the ovary largely, but not completely, coincides with that of R1 (fig. 1), suggesting both common and specific regulatory mechanisms in expression of R1 and R4. Unfortunately, transcriptional regulation of R1 or R4 has yet to be investigated. Elucidation of the regulatory mechanisms will reveal the spatiotemporal regulation of R1–R4 heterodimer in details, leading to the clarification of the biological significance of the species-specific heterodimer.

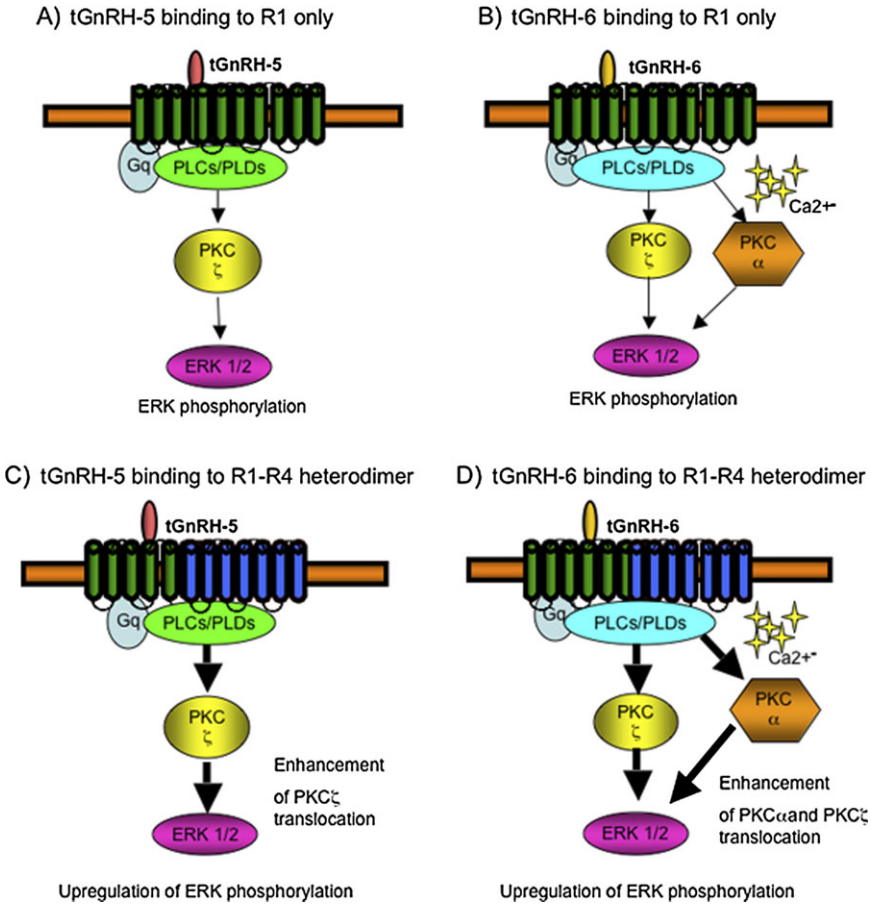

FIG. 8. Model of signaling modulation via R1–R4 heterodimerization. The activation of specific PKC subtypes, eventually leading to ERK phosphorylation, is differentially upregulated by heterodimerization between *Ciona* GnRH receptor, R1, and its orphan receptor paralog, R4 in a ligand-selective manner.

Gly^6 is evolutionarily conserved in all the GnRHs that trigger Ca^{2+} mobilization, including that of the octopus (Iwakoshi-Ukena et al. 2004; Kanda et al. 2006) and in the sea lamprey (Kavanaugh et al. 2008). A recent study indicated that protostomian GnRHs possess a Gly at the corresponding position of vertebrate GnRHs (Tsai and Zhang 2008). These findings suggest that ancestral GnRHs possess Gly^6. In *Ciona*, only tGnRH-6 possesses Gly^6 (Adams et al. 2003) and upregulates Ca^{2+} mobilization through R1 (Tello et al. 2005). Consequently, it is presumed that an R1–tGnRH-6 pair is the common GnRH signaling system, which originated from a common ancestor, and that other tGnRHs are *Ciona*-specific paralogs. Moreover, molecular phylogenetic analysis showed that R2, R3, and R4 were *Ciona*-specific GnRH receptor paralogs generated via gene duplication (Kusakabe et al. 2003; Tello et al. 2005). Combined with the findings that R1, R2, and R3 mediate differential signaling pathways with different ligand specificity (Tello et al. 2005), the ligand-selective modulation of multiple signaling pathways by the R1–R4 heterodimer is implicated with the molecular and functional evolution of *Ciona* GnRHergic systems. It is noteworthy that ascidians lack a hypothalamic–pituitary–periphery endocrine system, which is essentially conserved in vertebrates (Campbell et al. 2004; Satake and Kawada 2006). These findings support the view that ascidians lack a GnRHergic endocrine hypothalamic–pituitary–ovary axis, which is a prerequisite for appropriate reproductive function in vertebrates, and thus, tGnRHs do not act as a hypothalamic hormone. Instead, tGnRHergic neurons are directly projected to the ovary (Terakado 2001; Adams et al. 2003), and Ci-GnRHRs are expressed in ovarian cells (fig. 1). These results indicate that tGnRHs are involved in the regulation of ovarian functions in an exclusively neuropeptidergic fashion. Collectively, it is presumed that the modulation of multiple signaling pathways by the R1–R4 heterodimer, in concert with multiplication of tGnRHs and Ci-GnRHRs, enables spatiotemporal fine-tuning of the primitive neuropeptidergic GnRH signaling pathways, which is comparable with the hormonal GnRHergic systems in vertebrates. Furthermore, considering the fact that several species-specific GnRH and/or GnRHR forms have been identified in various species and the possibility that species-specific orphan GPCRs are present, we presume that heterodimerization of GPCRs, including GnRHRs, with their orphan subtypes has led to the evolution of species-specific fine-tuning of biological functions of signaling molecules.

In conclusion, we have substantiated a novel ligand-dependent modulation of GPCR functions through heterodimerization with an orphan receptor paralog. The present

study originally shows that GPCR heterodimerization confers functional diversity on signaling mechanisms widely conserved in various organisms and presumes the presence of species-specific GPCR heterodimer–directed signaling modulatory systems in any other organisms including human.

Supplementary Material

Supplementary tables S1 and S2, figures S1 and S2, and legends to the supplementary figures are available at *Molecular Biology and Evolution* online (http://www.mbe.oxfordjournals.org/).

Acknowledgments

The authors are grateful to Tomoe Kitao for technical advise. We also thank Kazuko Hirayama and all members of Maizuru Fisheries Research Station for cultivation of the ascidians. All ascidians were provided by Kyoto University through the National Bio-Resource Project of the Ministry of Education, Culture, Sports, Science and Technology, Japan. This study is in part financially supported by Japan Society for the Promotion of Science (to T.S.).

References

Adams BA, Tello J, Erchegyi J, Warby C, Hong DJ, Akinsanya KO, Mackie GO, Vale W, Rivier JE, Sherwood NM. 2003. Six novel gonadotropin-releasing hormones are encoded as triplets on each of two genes in the protochordate, *Ciona intestinalis*. *Endocrinology* 144:1907–1919.

Ando H, Urano A. 2005. Molecular regulation of gonadotropin secretion by gonadotropin-releasing hormone in salmonid fishes. *Zoolog Sci*. 22:379–389.

Aoyama M, Kawada T, Fujie M, Hotta K, Sakai T, Sekiguchi T, Oka K, Satoh N, Satake H. 2008. A novel biological role of tachykinins as an up-regulator of oocyte growth: identification of an evolutionary origin of tachykininergic functions in the ovary of the ascidian, *Ciona intestinalis*. *Endocrinology* 149:4346–4356.

Campbell RK, Satoh N, Degnan BM. 2004. Piecing together evolution of the vertebrate endocrine system. *Trends Genet*. 20:359–366.

Caunt CJ, Finch A, Sedgley KR, McArdle CA. 2006. GnRH receptor signalling to ERK: kinetics and compartmentalization. *Trends Endocrinol Metab*. 17:308–313.

Dobkin-Bekman M, Naidich M, Pawson AJ, Millar RP, Seger R, Naor Z. 2006. Activation of mitogen-activated protein kinase (MAPK) by GnRH is cell-context dependent. *Mol Cell Endocrinol*. 252:184–190.

Farshori PQ, Shah BH, Arora KK, Martinez-Fuentes A, Catt KJ. 2003. Activation and nuclear translocation of PKCdelta, Pyk2 and ERK1/2 by gonadotropin releasing hormone in HEK293 cells. *J Steroid Biochem Mol Biol*. 85:337–347.

Iwakoshi-Ukena E, Ukena K, Takuwa-Kuroda K, Kanda A, Tsutsui K, Minakata H. 2004. Expression and distribution of octopus gonadotropin-releasing hormone in the central nervous system and peripheral organs of the octopus (*Octopus vulgaris*) by in situ hybridization and immunohistochemistry. *J Comp Neurol*. 477:310–323.

Kah O, Lethimonier C, Somoza G, Guilgur LG, Vaillant C, Lareyre JJ. 2007. GnRH and GnRH receptors in metazoa: a historical, comparative, and evolutive perspective. *Gen Comp Endocrinol*. 153:346–364.

Kanda A, Takahashi T, Satake H, Minakata H. 2006. Molecular and functional characterization of a novel gonadotropin-releasing-hormone receptor isolated from the common octopus (*Octopus vulgaris*). *Biochem J*. 395:125–135.

Kavanaugh SI, Nozaki M, Sower SA. 2008. Origins of gonadotropin-releasing hormone (GnRH) in vertebrates: identification of a novel GnRH in a basal vertebrate, the sea lamprey. *Endocrinology* 149:3860–3869.

Kawada T, Aoyama M, Okada I, Sakai T, Sekiguchi T, Ogasawara M, Satake H. 2009. A novel inhibitory gonadotropin-releasing hormone-related neuropeptide in the ascidian, *Ciona intestinalis*. *Peptides*. 30:2200–2205.

Kratzmeier M, Poch A, Mukhopadhyay AK, McArdle CA. 1996. Selective translocation of non-conventional protein kinase C isoenzymes by gonadotropin-releasing hormone (GnRH) in the gonadotrope-derived alpha T3-1 cell line. *Mol Cell Endocrinol*. 118:103–111.

Kusakabe T, Mishima S, Shimada I, Kitajima Y, Tsuda M. 2003. Structure, expression, and cluster organization of genes encoding gonadotropin-releasing hormone receptors found in the neural complex of the ascidian *Ciona intestinalis*. *Gene* 322:77–84.

Levoye A, Dam J, Ayoub MA, Guillaume JL, Couturier C, Delagrange P, Jockers R. 2006. The orphan GPR50 receptor specifically inhibits MT1 melatonin receptor function through heterodimerization. *EMBO J*. 25:3012–3023.

Levoye A, Dam J, Ayoub MA, Guillaume JL, Jockers R. 2006. Do orphan G-protein-coupled receptors have ligand-independent functions? New insights from receptor heterodimers. *EMBO Rep*. 7:1094–1098.

Lindemans M, Liu F, Janssen T, Husson SJ, Mertens I, Gäde G, Schoofs L. 2009. Adipokinetic hormone signaling through the gonadotropin-releasing hormone receptor modulates egg-laying in *Caenorhabditis elegans*. *Proc Natl Acad Sci U S A*. 106:1642–1647.

Milasta S, Pediani J, Appelbe S, Trim S, Wyatt M, Cox P, Fidock M, Milligan G. 2006. Interactions between the Mas-related receptors MrgD and MrgE alter signalling and trafficking of MrgD. *Mol Pharmacol*. 69:479–491.

Millar RP, Lu ZL, Pawson AJ, Flanagan CA, Morgan K, Maudsley SR. 2004. Gonadotropin-releasing hormone receptors. *Endocr Rev*. 25:235–275.

Millar RP, Pawson AJ, Morgan K, Rissman EF, Lu ZL. 2008. Diversity of actions of GnRHs mediated by ligand-induced selective signaling. *Front Neuroendocrinol*. 29:17–35.

Milligan G, Smith NJ. 2007. Allosteric modulation of heterodimeric G-protein-coupled receptors. *Trends Pharmacol Sci*. 12:615–620.

Sasakura Y, Yamada L, Takatori N, Satou Y, Satoh N. 2003. A genomewide survey of developmentally relevant genes in *Ciona intestinalis*. VII. Molecules involved in the regulation of cell polarity and actin dynamics. *Dev Genes Evol*. 213:273–283.

Satake H, Kawada T. 2006. Neuropeptides, hormones, and their receptors in ascidians. In: Satake H, editor. Invertebrate neuropeptides and hormones: basic knowledge and recent advances. Kerala (India): Transworld Research Network. p. 253–276.

Satake H, Ogasawara M, Kawada T, Masuda K, Aoyama M, Minakata H, Chiba T, Metoki H, Satou Y, Satoh N. 2004. Tachykinin and tachykinin receptor of an ascidian, *Ciona intestinalis*: evolutionary origin of the vertebrate tachykinin family. *J Biol Chem*. 279:53798–53805.

Satake H, Sakai T. 2008. Recent advances and perceptions in studies of heterodimerization between G protein-coupled receptors. *Protein Pept Lett*. 15:300–308.

Satou Y, Sasakura Y, Yamada L, Imai KS, Satoh N, Degnan B. 2003. A genomewide survey of developmentally relevant genes in *Ciona intestinalis*. V. Genes for receptor tyrosine kinase pathway and Notch signaling pathway. *Dev Genes Evol*. 213:254–263.

Shacham S, Harris D, Ben-Shlomo H, Cohen I, Bonfil D, Przedecki F, Lewy H, Ashkenazi IE, Seger R, Naor Z. 2001. Mechanism of

GnRH receptor signaling on gonadotropin release and gene expression in pituitary gonadotrophs. *Vitam Horm*. 63:63–90.

Shah BH, Soh JW, Catt KJ. 2003. Dependence of gonadotropin-releasing hormone-induced neuronal MAPK signaling on epidermal growth factor receptor transactivation. *J Biol Chem*. 278:2866–2875.

Tello JA, River J, Sherwood NM. 2005. Tunicate gonadotropin-releasing hormone (GnRH) peptides selectively activate *Ciona intestinalis* GnRH receptors and the green monkey type II GnRH receptor. *Endocrinology* 146:4061–4073.

Terakado K. 2001. Induction of gamete release by gonadotropin-releasing hormone in a protochordate. *Ciona intestinalis Gen Comp Endocrinol*. 124:277–284.

Tsai PS, Zhang L. 2008. The emergence and loss of gonadotropin-releasing hormone in protostomes: orthology, phylogeny, structure, and function. *Biol Reprod*. 79:798–805.